Nanoscale Science and Technology

Edited by

Robert W. Kelsall
The University of Leeds, UK

Ian W. Hamley
The University of Leeds, UK

and

Mark Geoghegan
The University of Sheffield, UK

John Wiley & Sons, Ltd

Nanoscale Science and Technology

Nanoscale Science and Technology

Edited by

Robert W. Kelsall
The University of Leeds, UK

Ian W. Hamley
The University of Leeds, UK

and

Mark Geoghegan
The University of Sheffield, UK

John Wiley & Sons, Ltd

 John Wiley & Sons Ltd, The Atrium, Southern Gate, Chichester,
West Sussex PO19 8SQ, England

Telephone (+44) 1243 779777

Email (for orders and customer service enquiries): cs-books@wiley.co.uk
Visit our Home Page on www.wiley.com

Other Wiley Editorial Offices

John Wiley & Sons Inc., 111 River Street, Hoboken, NJ 07030, USA

Jossey-Bass, 989 Market Street, San Francisco, CA 94103-1741, USA

Wiley-VCH Verlag GmbH, Boschstr. 12, D-69469 Weinheim, Germany

John Wiley & Sons Australia Ltd, 33 Park Road, Milton, Queensland 4064, Australia

John Wiley & Sons (Asia) Pte Ltd, 2 Clementi Loop #02-01, Jin Xing Distripark, Singapore 129809

John Wiley & Sons Canada Ltd, 22 Worcester Road, Etobicoke, Ontario, Canada M9W 1L1

Library of Congress Cataloging in Publication Data

Nanoscale science and technology / edited by Robert W. Kelsall,
Ian W. Hamley, Mark Geoghegan.
p. cm.
ISBN 0-470-85086-8 (cloth : alk. paper)
1. Nanotechnology. 2. Nanoscience. 3. Nanostructured materials—Magnetic properties.
I. Kelsall, Robert W. II. Hamley, Ian W. III. Geoghegan, Mark.
T174.7.N358 2005
620′.5—dc22

2004016224

British Library Cataloguing in Publication Data

A catalogue record for this book is available from the British Library

ISBN 0-470-85086-8 (HB)

Typeset in 10/12pt Times by Integra Software Services Pvt. Ltd, Pondicherry, India
Printed and bound in Great Britain by Antony Rowe Ltd, Chippenham, Wiltshire
This book is printed on acid-free paper responsibly manufactured from sustainable forestry in which at least two trees are planted for each one used for paper production.

Contents

List of contributors

EDITORS

Dr Robert W. Kelsall
Institute of Microwaves and Photonics
School of Electronic and Electrical Engineering
University of Leeds
Leeds LS2 9JT
United Kingdom
r.w.kelsall@leeds.ac.uk

Dr Ian W. Hamley
Centre for Self Organising Molecular Systems
University of Leeds
Leeds LS2 9JT
United Kingdom
I.W.Hamley@chemistry.leeds.ac.uk

Dr Mark Geoghegan
Department of Physics and Astronomy
University of Sheffield
Sheffield S3 7RH
United Kingdom
mark.geoghegan@sheffield.ac.uk

AUTHORS

Dr Rik Brydson
Institute for Materials Research
School of Process, Environmental and Materials Engineering
University of Leeds
Leeds LS2 9JT
United Kingdom
mtlrmdb@leeds.ac.uk

Prof. Mike R. J. Gibbs
Department of Engineering Materials
University of Sheffield
Sheffield S1 3JD
United Kingdom
M.R.Gibbs@Sheffield.ac.uk

Dr Martin Grell
Department of Physics and Astronomy
University of Sheffield
Sheffield S3 7RH
United Kingdom
m.grell@sheffield.ac.uk

Dr Chris Hammond
Institute for Materials Research
School of Process, Environmental and Materials Engineering
University of Leeds
Leeds LS2 9JT
United Kingdom
c.hammond@leeds.ac.uk

Prof. Richard Jones
Department of Physics and Astronomy
Hicks Building
University of Sheffield
Sheffield S3 7HF
United Kingdom
r.a.l.jones@sheffield.ac.uk

Prof. Graham Leggett
Department of Chemistry
University of Sheffield
Sheffield S3 7HF
United Kingdom
graham.leggett@umist.ac.uk

Dr David Mowbray
Department of Physics and Astronomy
University of Sheffield
Sheffield S3 7RH
United Kingdom
d.mowbray@sheffield.ac.uk

Dr Iain Todd
Department of Engineering Materials
University of Sheffield
Sheffield S1 3JD
United Kingdom
i.todd@sheffield.ac.uk

Preface

In the two years since we first started planning this book, so much has been written about nanotechnology that the subject really needs no introduction. Nanotechnology has been one of the first major new technologies to develop in the internet age, and as such has been the topic of thousands of unregulated, unrefereed websites, discussion sites and the like. In other words, much has been written, but not all is necessarily true. The press has also made its own, unique contribution: 'nanotechnology will turn us all into grey goo' makes for a good story (in some newspapers at least), and then there's the 1960s image of nanotechnology, still present today, of Raquel Welch transported in a nanosubmarine through the bloodstream of an unsuspecting patient. This book isn't about *any* of that! One thing that the recent press coverage of nanotechnology has achieved is to draw attention to the possible hazards which accompany any new technology and to pose relevant questions about the likely impact of the various facets of nanotechnology on our society. Whilst we would certainly encourage investigation and discussion of such issues, they do not fall within the remit of this book.

Nanoscale Science and Technology has been designed as an educational text, aimed primarily at graduate students enrolled on masters or PhD programmes, or indeed, at final year undergraduate or diploma students studying nanotechnology modules or projects. We should also mention that the book has been designed for students of the physical sciences, rather than the life sciences. It is based largely on our own masters course, the Nanoscale Science and Technology MSc, which has been running since 2001 and was one of the first postgraduate taught courses in Europe in this subject area. The course is delivered jointly by the Universities of Leeds and Sheffield, and was designed primarily by several of the authors of this book. As in designing the course, so in designing the book have we sought to present the breadth of scientific topics and disciplines which contribute to nanotechnology. The scope of the text is bounded by two main criteria. Firstly, we saw no need to repeat the fine details of established principles and techniques which are adequately covered elsewhere, and secondly, as a textbook, *Nanoscale Science and Technology* is intended to be read, in its entirety, over a period of one year. In consideration of the first of these criteria, each chapter has a bibliography indicating where more details of particular topics can be found.

The expertise of the authors ranges from electronic engineering, physics and materials science to chemistry and biochemistry, which we believe has helped us achieve both breadth and balance. That said, this book is inevitably our take on nanotechnology, and any other group of authors would almost certainly have a different opinion on what should be included and what should be emphasised. Also, in such a rapidly developing

field, our reporting is in danger of fast becoming out of date (one of our co-authors, who was the most efficient in composing his text, paid the rather undeserved penalty of having to make at least two sets of revisions simply to update facts and figures to reflect new progress in research). We should certainly be grateful to receive any information on errors or omissions.

Although most of the chapters have been written by different authors, we were keen that, to better fulfil its role as a textbook, this volume should read as one coherent whole rather than as a collection of individual monographs. To this end, not only have we as editors made numerous adjustments to improve consistency, and avoid duplication and omission, but in some places we have also made more substantial editorial changes. We should like to acknowledge the tolerance of our co-authors throughout this process. We are all still on speaking terms – just! It is not really necessary for us to tabulate in detail exactly who contributed what to each chapter in the final manuscript, except that we note that the nanostructured carbon section in Chapter 6 was provided by Rob Kelsall. Finally, we should like to acknowledge Terry Bambrook, who composed virtually all of the figures for chapters 1 and 2.

Robert W. Kelsall, Ian W. Hamley and Mark Geoghegan

Book cover acknowledgments

The nano images of silicon were taken by Dr Ejaz Huq and appear courtesy of the CCLRC Rutherford Appleton Laboratory Central Microstructure Facility; the images of carbon nanotubes appears courtesy of Z. Aslam, B. Rand and R. Brydson (University of Leeds); the image of a templated silica nanotube appears courtesy of J. Meegan, R. Ansell and R. Brydson (University of Leeds); the image of microwires is taken from E. Cooper, R. Wiggs, D. A. Hutt, L. Parker, G. J. Leggett and T. L. Parker, *J. Mater. Chem.* **7**, 435–441 (1997), reproduced by permission of the Royal Society of Chemistry, and the AFM images of block copolymers are adapted with permission from T. Mykhaylyk, O. O. Mykhaylyk, S. Collins and I. W. Hamley, *Macromolecules* **37**, 3369 (2004), copyright 2004 American Chemical Society.

Chapter authors

Chapter 1. Generic methodologies for nanotechnology: classification and fabrication
Rik M. Brydson and Chris Hammond

Chapter 2. Generic methodologies for nanotechnology: characterisation
Rik M. Brydson and Chris Hammond

Chapter 3. Inorganic semiconductor nanostructures
David Mowbray

Chapter 4. Nanomagnetic materials and devices
Mike R. J. Gibbs

Chapter 5. Processing and properties of inorganic nanomaterials
Iain Todd

Chapter 6. Electronic and electro-optic molecular materials and devices
Martin Grell

Chapter 7. Self-assembling nanostructured molecular materials and devices
Ian W. Hamley

Chapter 8. Macromolecules at interfaces and structured organic films
Mark Geoghegan and Richard A. L. Jones

Chapter 9. Bionanotechnology
Graham J. Leggett and Richard A. L. Jones

1

Generic methodologies for nanotechnology: classification and fabrication

1.1 INTRODUCTION AND CLASSIFICATION

1.1.1 What is nanotechnology?

Nanotechnology is the term used to cover the design, construction and utilization of functional structures with at least one characteristic dimension measured in nanometres. Such materials and systems can be designed to exhibit novel and significantly improved physical, chemical and biological properties, phenomena and processes as a result of the limited size of their constituent particles or molecules. The reason for such interesting and very useful behaviour is that when characteristic structural features are intermediate in extent between isolated atoms and bulk macroscopic materials; i.e., in the range of about 10^{-9} m to 10^{-7} m (1 to 100 nm), the objects may display physical attributes substantially different from those displayed by either atoms or bulk materials. Ultimately this can lead to new technological opportunities as well as new challenges.

1.1.2 Classification of nanostructures

As we have indicated above, a reduction in the spatial dimension, or confinement of particles or quasiparticles in a particular crystallographic direction within a structure generally leads to changes in physical properties of the system in that direction. Hence one classification of nanostructured materials and systems essentially depends on the number of dimensions which lie within the nanometre range, as shown in Figure 1.1: (a) systems confined in three dimensions, (b) systems confined in two dimensions, (c) systems confined in one dimension.

Nanoscale Science and Technology Edited by R. W. Kelsall, I. W. Hamley and M. Geoghegan

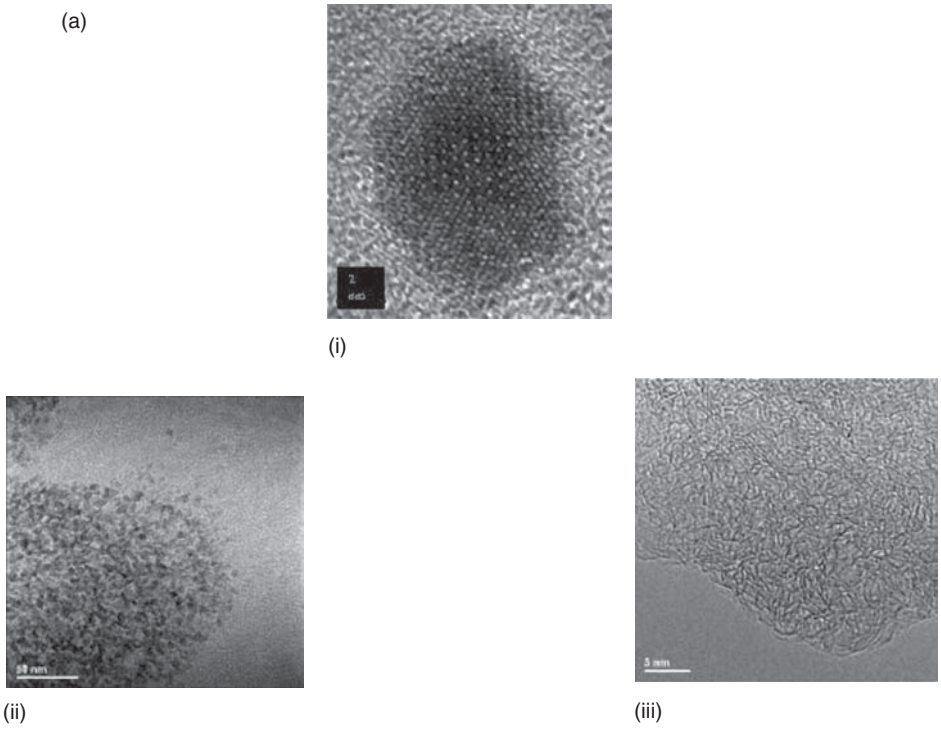

Figure 1.1 Classification of nanostructures. (a) Nanoparticles and nanopores (nanosized in three dimensions): (i) high-resolution TEM image of magnetic iron oxide nanoparticle, (ii) TEM image of ferritin nanoparticles in a liver biopsy specimen, and (iii) high-resolution TEM image of nanoporosity in an activated carbon). (b) Nanotubes and nanofilaments (nanosized in two dimensions): (i) TEM image of single-walled carbon nanotubes prepared by chemical vapour deposition, (ii) TEM image of ordered block copolymer film, and (iii) SEM image of silica nanotube formed via templating on a tartaric acid crystal. (c) Nanolayers and nanofilms (nanosized in one dimension): (i) TEM image of a ferroelectric thin film on an electrode, (ii) TEM image of cementite (carbide) layers in a carbon steel, and (iii) high-resolution TEM image of glassy grain boundary film in an alumina polycrystal. Images courtesy of Andy Brown, Zabeada Aslam, Sarah Pan, Manoch Naksata and John Harrington, IMR, Leeds

Nanoparticles and nanopores exhibit three-dimensional confinement (note that historically pores below about 100 nm in dimension are often sometimes confusingly referred to as micropores). In semiconductor terminology such systems are often called quasi-zero dimensional, as the structure does not permit free particle motion in any dimension.

Nanoparticles may have a random arrangement of the constituent atoms or molecules (e.g., an amorphous or glassy material) or the individual atomic or molecular units may be ordered into a regular, periodic crystalline structure which may not necessarily be the same as that which is observed in a much larger system (Section 1.3.1). If crystalline, each nanoparticle may be either a single crystal or itself composed of a number of different crystalline regions or grains of differing crystallographic orientations (i.e., polycrystalline) giving rise to the presence of associated grain boundaries within the nanoparticle.

(b)

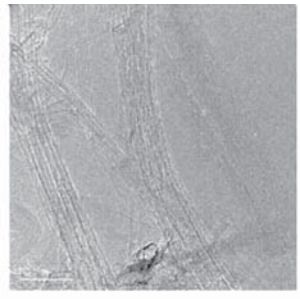

(i)

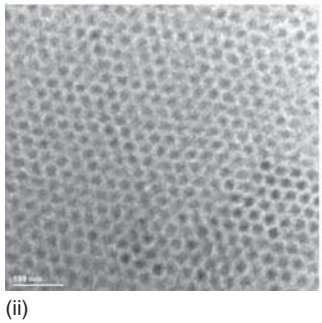

(ii)

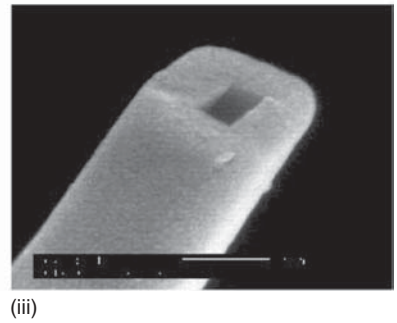

(iii)

(c)

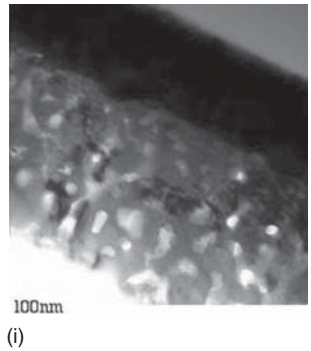

(i)

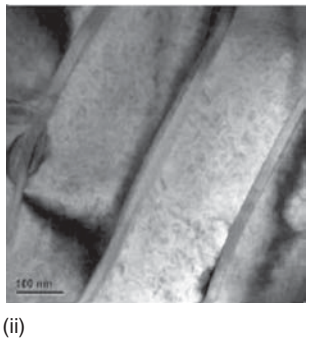

(ii)

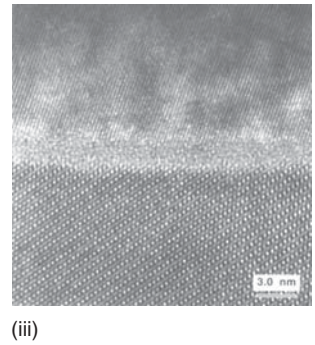

(iii)

Figure 1.1 Continued

Nanoparticles may also be quasi-crystalline, the atoms being packed together in an icosahedral arrangement and showing non-crystalline symmetry characteristics. Such quasi-crystals are generally only stable at the nanometre or, at most, the micrometre scale.

Nanoparticles may be present within another medium, such as nanometre-sized precipitates in a surrounding matrix material. These nanoprecipitates will have a specific morphology (e.g., spherical, needle-shaped or plate-shaped) and may possess certain crystallographic orientation relationships with the atomic arrangement of the matrix depending on the nature (coherency) of the interface which may lead to coherency strains in the particle and the matrix. One such example is the case of self-assembled semiconductor quantum dots, which form due to lattice mismatch strain relative to the surrounding layers and whose geometry is determined by the details of the strain field (Chapter 3). Another feature which may be of importance for the overall transport properties of the composite system is the connectivity of such nanometre-sized regions or, in the case of a nanoporous material, nanopore connectivity.

In three dimensions we also have to consider collections of consolidated nanoparticles; e.g., a nanocrystalline solid consisting of nanometre-sized crystalline grains each in a specific crystallographic orientation. As the grain size d of the solid decreases the proportion of atoms located at or near grain boundaries, relative to those within the interior of a crystalline grain, scales as $1/d$. This has important implications for properties in ultrafine-grained materials which will be principally controlled by interfacial properties rather than those of the bulk.

Systems confined in two dimensions, or quasi-1D systems, include nanowires, nanorods, nanofilaments and nanotubes: again these could either be amorphous, single-crystalline or polycrystalline (with nanometre-sized grains). The term 'nanoropes' is often employed to describe bundles of nanowires or nanotubes.

Systems confined in one dimension, or quasi-2D systems, include discs or platelets, ultrathin films on a surface and multilayered materials; the films themselves could be amorphous, single-crystalline or nanocrystalline.

Table 1.1 gives examples of nanostructured systems which fall into each of the three categories described above. It can be argued that self-assembled monolayers and multi layered Langmuir–Blodgett films (Section 1.4.3.1) represent a special case in that they represent a quasi-2D system with a further nanodimensional scale within the surface film caused by the molecular self-organization.

1.1.3 Nanoscale architecture

Nanotechnology is the design, fabrication and use of nanostructured systems, and the growing, shaping or assembling of such systems either mechanically, chemically or biologically to form nanoscale architectures, systems and devices. The original vision of Richard Feynman[1] was of the 'bottom-up' approach of fabricating materials and devices at the atomic or molecular scale, possibly using methods of self-organization and self-assembly of the individual building blocks. An alternative 'top-down' approach is the

[1] R. Feynman, There's plenty of room at the bottom, *Eng. Sci.* **23**, 22 (1960) reprinted in *J. Micromech Systems* **1**, 60 (1992).

Table 1.1 Examples of reduced-dimensionality systems

3D confinement
Fullerenes
Colloidal particles
Nanoporous silicon
Activated carbons
Nitride and carbide precipitates in high-strength low-alloy steels
Semiconductor particles in a glass matrix for non-linear optical components
Semiconductor quantum dots (self-assembled and colloidal)
Quasi-crystals
2D confinement
Carbon nanotubes and nanofilaments
Metal and magnetic nanowires
Oxide and carbide nanorods
Semiconductor quantum wires
1D confinement
Nanolaminated or compositionally modulated materials
Grain boundary films
Clay platelets
Semiconductor quantum wells and superlattices
Magnetic multilayers and spin valve structures
Langmuir–Blodgett films
Silicon inversion layers in field effect transistors
Surface-engineered materials for increased wear resistance or corrosion resistance

ultraminiaturization or etching/milling of smaller structures from larger ones. These methods are reviewed in Section 1.4. Both approaches require a means of visualizing, measuring and manipulating the properties of nanostructures; computer-based simulations of the behaviour of materials at these length scales are also necessary. This chapter provides a general introduction to the preparation and properties of nanostructures, whilst the subsequent chapters give greater detail on specific topics.

1.2 SUMMARY OF THE ELECTRONIC PROPERTIES OF ATOMS AND SOLIDS

To understand the effects of dimensionality in nanosystems, it is useful to review certain topics associated with the constitution of matter, ranging from the structure of the isolated atom through to that of an extended solid.

1.2.1 The isolated atom

The structure of the atom arises as a direct result of the wave–particle duality of electrons, which is summarized in the de Broglie relationship, $\lambda = h/m_e v$, where λ is the (electron) wavelength, m_e is the (electron) mass, v is the velocity and

$h = 6.63 \times 10^{-34}$ J s is the Planck constant. The wave–particle duality of the electron means that an electron behaves both as a wave (i.e., it is extended over space and has a wavelength and hence undergoes wave-like phenomena such as diffraction) and a particle (i.e., it is localized in space and has a position, a velocity and a kinetic energy). This is conveniently summarized in the idea of a wave packet a localized wave that is effectively the summation of a number of different waves of slightly differing wavelengths.

Using these ideas we come to our first model of the atom, the Rutherford–Bohr model. Here the small central nucleus of the atom consists of positively charged protons and (neutral) neutrons. Electrons orbit the nucleus in stable orbits. The allowed, stable orbits are those in which the electron wavelength, given by the de Broglie formula, is an integral multiple n of the circumference of the orbit r:

$$2\pi r = n\lambda = \frac{nh}{m_e v}. \tag{1.1}$$

This implies that

$$m_e v r = \frac{nh}{2\pi}, \tag{1.2}$$

in otherwords, the angular momentum $m_e vr$ is quantized in that it is an integral multiple of $h/2\pi$.

The Bohr model leads to the idea that only certain electron orbits or shells are allowed by this quantization of angular momentum (i.e., the value of n). The Bohr shells in an atom are labelled according to the quantum number, n, and are given the spectroscopic labels K, L, M, N, etc. (where $n = 1, 2, 3, 4, \ldots$). To understand the form of the periodic table of elements, it is necessary to assume that each Bohr shell can contain $2n^2$ electrons. For instance, a K shell ($n = 1$) can contain 2 electrons, whereas an L shell ($n = 2$) can accommodate 8 electrons. As well as having a distinct form and occupancy, each shell also has a corresponding well-defined energy. It is usual to define the zero of the energy scale (known as the vacuum level) as the potential energy of a free electron far from the atom. In order to correspond with atomic emission spectra measured experimentally, the energies of these levels E_n are then negative (i.e., the electrons are bound to the atom) and are proportional to $1/n^2$. Such a simplified picture of the structure of an isolated Mg atom and the associated energy level diagram are shown in Figure 1.2.

A much more sophisticated model of the atom considers the wave-like nature of the electrons from the very beginning. This uses wave mechanics or quantum mechanics.

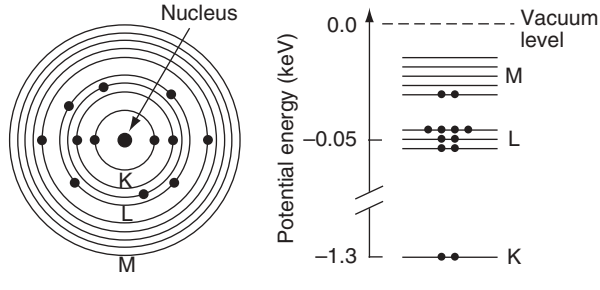

Figure 1.2 Bohr shell description of an Mg atom and the associated energy level diagram

Here each electron is described by a wavefunction ψ which is a function of spatial position (x,y,z) and, in general, of time. Physically $|\psi|^2$ represents the probability of finding the electron at any point. To work out the energy of each electron, we need to solve the Schrödinger equation which, in the time-independent case, takes the form

$$-\frac{\hbar^2}{2m_e}\nabla^2\psi + V(x,y,z)\psi = E\psi\,, \tag{1.3}$$

where V(x,y,z) describes the potential energy function in the environment of the electron. Solution of the Schrödinger equation, under certain boundary conditions, leads to a set of solutions for the allowed wavefunctions ψ_n of the atomic electrons together with their associated energies E_n.

This equation can only be solved analytically for the case of the hydrogen atom, where there is only one electron moving in the potential of a single proton, the hydrogen nucleus. Only a certain set of electronic wavefunctions and associated energy levels fulfil this Schrödinger equation. The wavefunctions may be expressed as a radial part, governing the spatial extent of the wavefunction, multiplied by a spherical harmonic function which determines the shape. The allowed wavefunctions form the electron orbitals, which we term 1s, 2s, 2p, 3s, 3p, 3d, etc. (here $1, 2, 3, \ldots$ are alternative labels for $\mathrm{K}, \mathrm{L}, \mathrm{M}, \ldots$). These allowed wavefunctions now depend on not just one quantum number but four: n, l, m and s. These numbers may be summarized as follows:

- n is the principal quantum number; it is like the quantum number used for the case of Bohr shells ($n = 1, 2, 3, \ldots$).
- l is the angular momentum quantum number; it can vary from $l = 0, 1, 2, \ldots, (n-1)$. The value of l governs the orbital shape of the subshell: $l = 0$ is an s orbital, which is spherical; $l = 1$ is a p orbital, which has a dumbbell shape; while $l = 2$ is a d orbital, which has a more complex shape such as a double dumbbell.
- m is the magnetic quantum number; it can vary from $m = 0, \pm1, \ldots, \pm l$. The value of m governs the spatial orientation of the different orbitals within a subshell; i.e., there are three p orbitals ($l = 1$) p_x, p_y, and p_z corresponding to the three values of m which are 0, +1 and −1. In the absence of a magnetic field, all these orbitals within a particular subshell will have the same energy.
- s is the spin quantum number which, for an electron, can take the values $\pm1/2$. Each (n, l, m) orbital can contain two electrons of opposite spin due to the Pauli exclusion principle, which states that no two electrons can have the same four quantum numbers.

Using this identification in terms of the quantum numbers, each electron orbital in an atom therefore has a distinct combination of energy, shape and direction (x, y, z) and can contain a maximum of two electrons of opposite spin.

In an isolated atom, these localized electronic states are known as Rydberg states and may be described in terms of simple Bohr shells or as combinations of the three quantum numbers n, l and m known as electron orbitals. The Bohr shells (designated $\mathrm{K}, \mathrm{L}, \mathrm{M}, \ldots$) correspond to the principal quantum numbers n equal to 1, 2, 3, etc. Within each of these shells, the electrons may exist in $(n-1)$ subshells (i.e., s, p, d, or f subshells, for which the angular momentum quantum number l equals 0, 1, 2, 3, respectively).

The occupation of the electronic energy levels depends on the total number of electrons in the atom. In the hydrogen atom, which contains only one electron, the set of Rydberg states is almost entirely empty except for the lowest-energy 1s level which is half full. As we go to higher energies, the energy spacing between these states becomes smaller and smaller and eventually converges to a value known as the vacuum level ($n = \infty$), which corresponds to the ionization of the inner-shell electron. Above this energy the electron is free of the atom and this is represented by a continuum of empty electronic states. In fact, the critical energy to ionize a single isolated hydrogen atom is equal to 13.61 eV and this quantity is the Rydberg constant.

This description is strictly only true for hydrogen; however, other heavier atoms are found to have similar wavefunction (hydrogenic-like) solutions, which ultimately leads to the concept of the periodic table of elements, as each atom has more and more electrons which progressively fill the allowed energy levels. This is shown for a magnesium atom in Figure 1.2. The chemical properties of each atom are then principally determined by the number of valence electrons in the outermost electron shell which are relatively loosely bound and available for chemical reaction with other atomic species.

1.2.2 Bonding between atoms

One way to picture the bonding between atoms is to use the concept of Molecular Orbital (MO) Theory. MO theory considers the electron wavefunctions of the individual atoms combining to form molecular wavefunctions (or molecular orbitals as they are known). These orbitals, which are now delocalized over the whole molecule, are then occupied by all the available electrons from all the constituent atoms in the molecule. Molecular orbitals are really only formed by the wavefunctions of the electrons in the outermost shells (the valence electrons); i.e., those which significantly overlap in space as atoms become progressively closer together; the inner electrons remain in what are essentially atomic orbitals bound to the individual atoms.

A simple one-electron molecule is the H_2^+ ion, where we have to consider the interactions (both attractive and repulsive) between the single electron and two nucleii. The Born–Oppenheimer approximation regards the nuclei as fixed and this simplifies the Hamiltonian used in the Schrödinger equation for the molecular system. For a one-electron molecule, the equation can be solved mathematically, leading to a set of molecular wavefunctions ψ which describe molecular orbitals and depend on a quantum number λ which specifies the angular momentum about the internuclear axis. Analogous to the classification of atomic orbitals (AOs) in terms of angular momentum l as s, p, d, etc., the MOs may be classified as σ, π, δ depending on the value of λ ($\lambda = 0, 1, 2$, respectively). Very simply a σ MO is formed from the overlap (actually a linear combination) of AOs parallel to the bond axis, whereas a π MO results from the overlap of AOs perpendicular to the bond axis. For the H_2^+ ion, the two lowest-energy solutions are known as $1s\sigma_g$ and $1s\sigma_u$. Here 1s refers to the original atomic orbitals; the subscripts g and u refer to whether the MO is either symmetrical or non-symmetrical with respect to inversion about a line drawn between the nucleii (viz. an even or odd mathematical function). This is shown in figure 1.3.

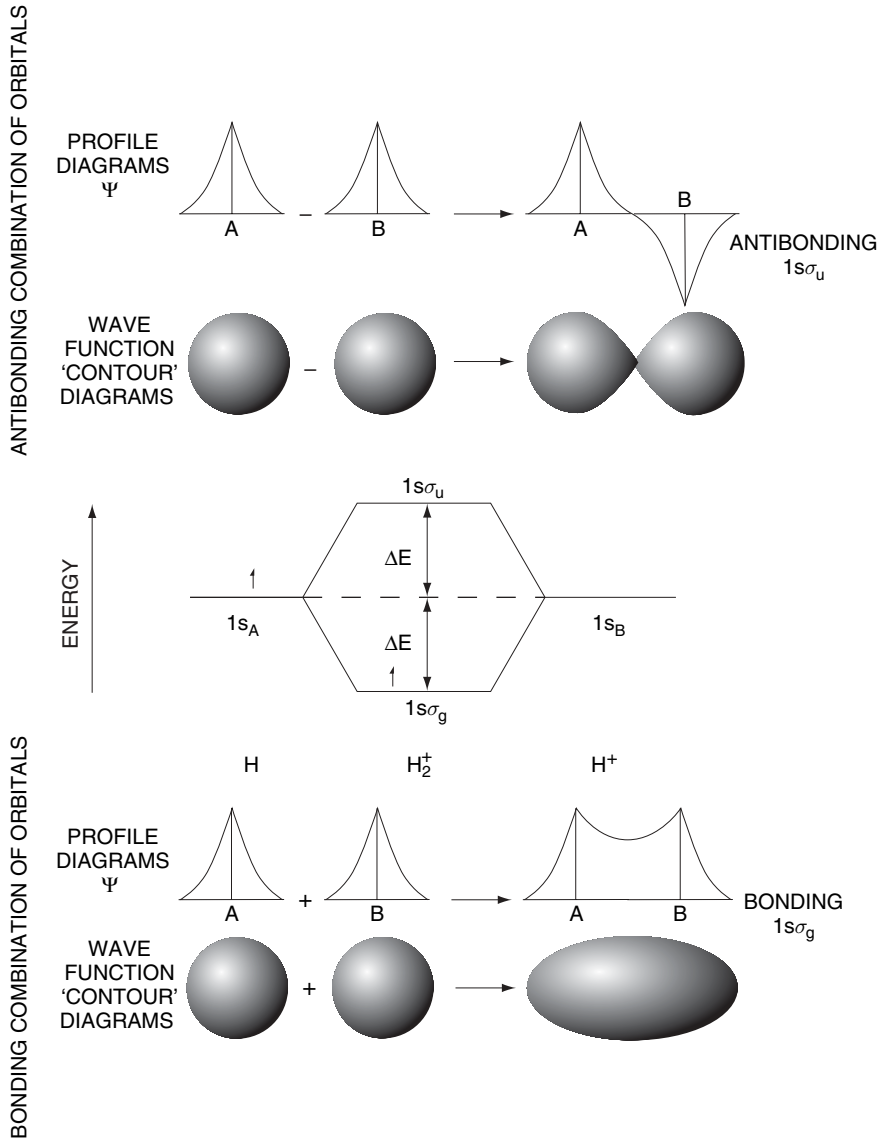

Figure 1.3 Molecular orbital description and energy level diagram for an H_2^+ ion

As can be seen the electron density is concentrated between the nuclei for the $1s\sigma_g$ MO, which is known as a bonding orbital since the energy of the molecular wavefunction is lower (i.e., more stable) than the corresponding isolated atomic wavefunctions. Conversely, the electron density is diminished between the nuclei for $1s\sigma_u$, which is known as an antibonding orbital since the energy of the molecular wavefunction is higher (i.e., less stable) than the corresponding isolated atomic wavefunction.

More generally, it is necessary to be able to solve the Schrödinger equation for molecules containing more than one electron. One way to do this is to use approximate

solutions similar to those obtained for the hydrogen atom, since when an electron is near a particular nucleus it will have a hydrogen-like form. Using this approach we can then construct a set of molecular orbitals from a linear combination of atomic orbitals (LCAO). For instance, as shown in Figure 1.4, the $1s\sigma_g$ bonding MO is formed from the in-phase overlap (i.e., addition) of two 1s atomic orbitals, whereas the $1s\sigma_u$ antibonding MO is formed from the out of-phase overlap (i.e., subtraction) of two 1s atomic orbitals. Similar considerations apply to overlap of p orbitals, although now these may form both σ and π bonding and antibonding MOs.

The stability of simple diatomic molecules such as H_2, H_2^- and He_2 depends on the relative filling of the bonding and antibonding MOs; e.g., H_2^- contains three electrons, two of which fill the bonding MO ($1s\sigma_g$ level) while the third enters the antibonding MO ($1s\sigma_u$ level); consequently, the overall bond strength is approximately half that in H_2. Meanwhile He_2 is unstable as there are an equal number of electrons in bonding MOs as in antibonding MOs. The same principles apply to more complicated diatomic molecules. However, if the atoms are different then the energy levels of the electrons associated with the constituent atoms will also be different and this will lead to an asymmetry in the MO energy level diagram.

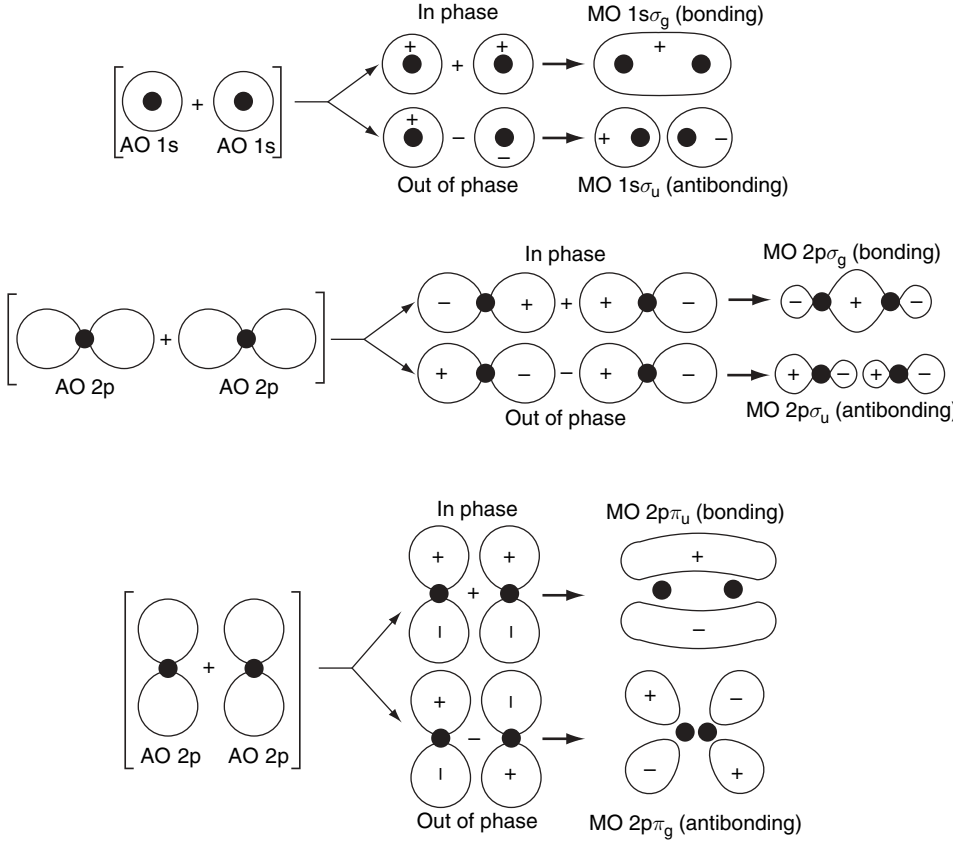

Figure 1.4 Formation of molecular orbitals from a linear combination of atomic orbitals; the + and − signs indicate the signs (phases) of the wavefunctions

For polyatomic molecules such as BF_3 a greater variety of molecular orbitals can be formed. MO theory emphasizes the delocalized nature of the electron distribution, so in general these MOs are extended over not just two, but all the constituent atoms. The total number of MOs (bonding, antibonding or non-bonding) is equal to the number of valence atomic orbitals used to construct them.

1.2.3 Giant molecular solids

When atoms come into close proximity with other atoms in a solid, most of the electrons remain localized and may be considered to remain associated with a particular atom. However, some outer electrons will become involved in bonding with neighbouring atoms. Upon bonding the atomic energy level diagram is modified. Briefly, the well-defined outer electron states of the atom overlap with those on neighbouring atoms and become broadened into energy bands. One convenient way of picturing this is to envisage the solid as a large molecule. Figure 1.5 shows the effect of increasing the number of atoms on the electronic energy levels of a one-dimensional solid (a linear chain of atoms).

For a simple diatomic molecule, as discussed previously, the two outermost atomic orbitals (AOs) overlap to produce two molecular orbitals (MOs) which can be viewed as a linear combination of the two constituent atomic orbitals. As before, the bonding MO is formed from the in-phase overlap of the AOs and is lower in energy than the corresponding AOs, whereas the other MO, formed from the out-of-phase overlap, is higher in energy than the corresponding AOs and is termed an antibonding MO. Progressively increasing the length of the molecular chain increases the total number of MOs, and gradually these overlap to form bands of allowed energy levels which are separated by forbidden energy regions (band gaps). These band gaps may be thought of as arising from the original energy gaps between the various atomic orbitals of the isolated atoms.

Note that the broadening of atomic orbitals into energy bands as the atoms are brought closer together to form a giant molecular solid can sometimes result in the overlapping of energy bands to give bands of mixed (atomic) character. The degree to which the orbitals are concentrated at a particular energy is reflected in a quantity known as the density of states (DOS) $N(E)$, where $N(E)\,dE$ is the number of allowed

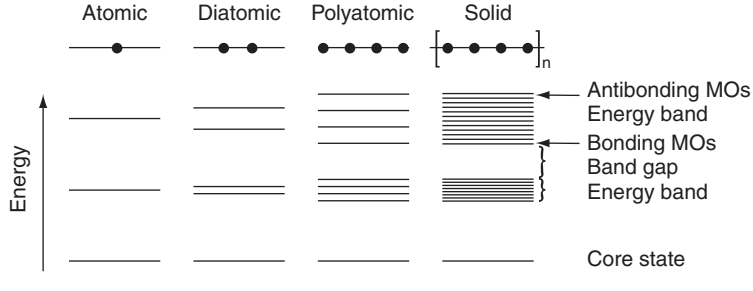

Figure 1.5 Electron energy level diagram for a progressively larger linear chain of atoms showing the broadening of molecular orbitals into energy bands for a one-dimensional solid

energy levels per unit volume of the solid in the energy range between E and $E + dE$. As in a simple molecule, each MO energy level in the energy band can accommodate two electrons of opposite spin. The total number of electrons from all the interacting atomic orbitals in the large molecule fill this set of MOs, the highest occupied energy level being known as the Fermi level E_F. The sum of the energies of all the individual electrons in the large molecule gives the total energy of the system, which gives a measure of the stability of the atomic arrangement in terms of the system free energy.

1.2.4 The free electron model and energy bands

An alternative view of the electronic band structure of solids is to consider the electron waves in a periodic crystalline potential. The starting point for this approach is the Drude–Lorentz free electron model for metals. In this model a metallic solid is considered as consisting of a close packed lattice of positive cations surrounded by an electron sea or cloud formed from the ionization of the outer shell (valence) electrons. We can then treat the valence electrons as if they were a gas inside a container and use classical kinetic gas theory. This works best for the electropositive metals of Groups I and II as well as aluminium (the so-called free electron metals) and can explain many of the fundamental properties of metals such as high electrical and thermal conductivities, optical opacity, reflectivity, ductility and alloying properties.

However, a more realistic approach is to treat the free electrons in metals quantum mechanically and consider their wave-like properties. Here the free valence electrons are assumed to be constrained within a potential well which essentially stops them from leaving the metal (the 'particle-in-a-box' model). The box boundary conditions require the wavefunctions to vanish at the edges of the crystal (or 'box'). The allowed wavefunctions given by the Schrödinger equation then correspond to certain wavelengths as shown in Figure 1.6. For a one-dimensional box of length L, the permitted wavelengths are $\lambda_n = 2L/n$, where $n = 1, 2, 3 \ldots$ is the quantum number of the state; the permitted wavevectors $k_n = 2\pi/\lambda$ are given by $k_n = n\pi/L$.

This simple particle-in-a-box model results in a set of wavefunctions given by

$$\psi_n = (2/L)^{1/2} \sin(n\pi x/L), \tag{1.4}$$

where $n = 1, 2, 3 \ldots .$, and for each n the corresponding energy of the electronic level is

$$E_n = \frac{n^2 h^2}{8mL^2}. \tag{1.5}$$

E_n represents solely kinetic energy since the potential energy is assumed to be zero within the box. Thus there is a parabolic relationship between E_n and n, and therefore between E_n and k since k depends directly on n as described above. The permitted energy levels on this parabola are discrete (i.e., quantized): however in principle the size of L for most metal crystals (ranging from microns to millimetres or even centimetres) means that the separation between levels is very small compared with the thermal energy $k_B T$,

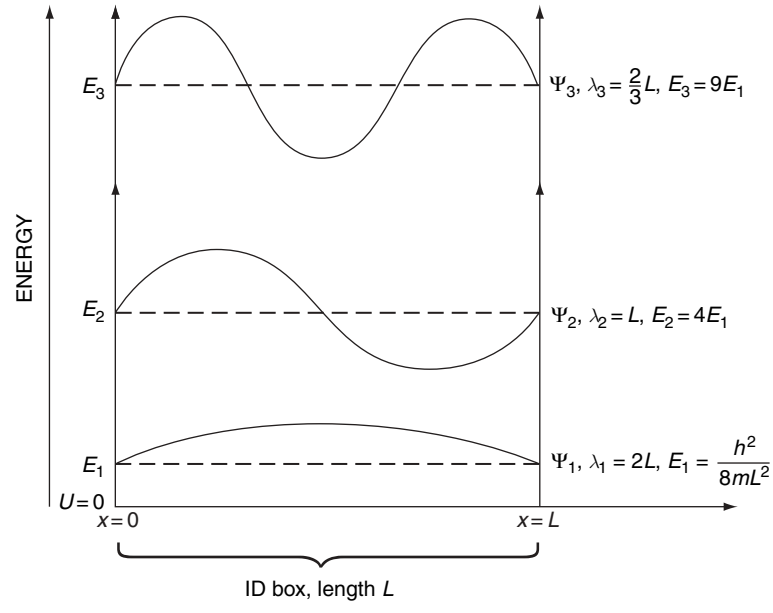

Figure 1.6 Energy level diagram also showing the form of some of the allowed wavefunctions for an electron confined to a one-dimensional potential well

and we can regard the energy distribution as almost continuous (quasi-continuous) so that the levels form a band of allowed energies as shown in figure 1.7.

Note that as the electron becomes more localized (i.e., L decreases), the energy of a particular electron state (and more importantly the spacing between energy states) increases; this has important implications for bonding and also for reduced-dimensionality or quantum-confined systems which are discussed later.

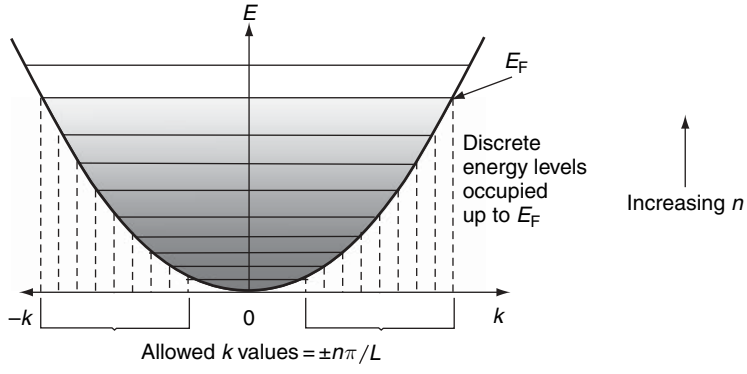

Figure 1.7 Schematic version of the parabolic relationship between the allowed electron wave vectors and the their energy for electrons confined to a one-dimensional potential well. Shaded energy regions represent those occupied with electrons

1.2.5 Crystalline solids

The above arguments may be extended from one to three dimensions to consider the electronic properties of bulk crystalline solids. For a perfectly ordered three dimensional crystal, the periodic repetition of atoms (or molecules) along the one dimensional linear chain considered in Section 1.2.2 is replaced by the periodic repetition of a *unit cell* in all three dimensions. The unit cell contains atoms arranged in the characteristic configuration of the crystal, such that contiguous replication of the unit cell throughout all space is sufficient to generate the entire crystal structure. In otherwords, the crystal has translational symmetry, and the crystal structure may be generated by translations of the unit cell in all three dimensions. Translation symmetry in a periodic structure is a so-called discrete symmetry, because only certain translations – those corresponding to integer multiples of the *lattice translation vectors* derived from the unit cell – lead to symmetry-equivalent points. (This may be contrasted with the case of empty space, which displays a continuous translation symmetry because *any* translation leads to a symmetry-equivalent point.) Common unit cells are simple cubic, face centred cubic, body centred cubic, and the diamond structure, which comprises two interlocking face-centred cubic lattices. However, in general, the lattice spacing may be different along the different principal axes, giving rise to the orthorhombic and tetragonal unit cells, and sides of the unit cell may not necessarily be orthogonal, such as in the hexagonal unit cell (refer to the Bibliography for further reading on this topic).

Generally, symmetries generate conservation laws; this is known as *Noether's theorem*. The continuous translation symmetry of empty space generates the law of momentum conservation; the weaker discrete translation symmetry in crystals leads to a weaker quasi-conservation law for quasi- or crystal momentum. An important consequence of discrete translation symmetry for the electronic properties of crystals is *Bloch's theorem*, which is described below.

1.2.6 Periodicity of crystal lattices

The three dimensional periodicity of the atomic arrangement in a crystal gives rise to a corresponding periodicity in the internal electric potential due to the ionic cores. Incorporating this periodic potential into the Schrödinger equation results in allowed wavefunctions that are modulated by the lattice periodicity. Bloch's theorem states that these wavefunctions take the form of a plane wave (given by $\exp(\mathrm{i}\mathbf{k}.\mathbf{r})$) multiplied by a function which has the same periodicity as the lattice; i.e.,

$$\psi(\mathbf{r}) = u_k(\mathbf{r}) \exp(\mathrm{i}\mathbf{k}.\mathbf{r}), \tag{1.6}$$

where the function $u_k(\mathbf{r})$ has the property $u_k(\mathbf{r}+\mathbf{T}) = u_k(\mathbf{r})$, for any lattice translation vector $\mathbf{T}$. Such wavefunctions are known as Bloch functions, and represent travelling waves passing through the crystal, but with a form modified periodically by the crystal potential due to each atomic site. For a one dimensional lattice of interatomic spacing a, these relationships reduce to

$$\psi(x) = u_k(x) \exp(\mathrm{i}kx) \tag{1.7}$$

with $u_k(x+na)=u_k(x)$ for any integer n. Now, if we impose periodic boundary conditions at the ends of the chain of atoms of length $L=Na$:

$$\psi(Na)=\psi(0), \tag{1.8}$$

we find that

$$u_k(Na)\exp(\mathrm{i}kNa)=u_k(0), \tag{1.9}$$

from which $\exp(\mathrm{i}kNa)=1$, which has the solutions

$$k=\pm 2n\pi/Na=\pm 2n\pi/L \tag{1.10}$$

for integer n. This result has two important consequences: firstly, it tells us that the difference between consecutive k values is always $2\pi/L$, which can be interpreted as representing the volume (or properly, in this simplified one dimensional case, the *length*) of **k**-space occupied by each wavevector state. Applying this argument to each dimension in turn gives, for a 3D crystal, a **k**-space volume of $8\pi^3/V$ occupied by each wavevector state, where $V=L^3$ is the crystal volume. Secondly, once the upper limit on n is determined, equation (1.10) will also tell us how many wavevector states are contained within each energy band. This point is examined below.

The lattice periodicity also gives rise to diffraction effects. Diffraction of X-rays in crystals is discussed in detail in Chapter 2, as an important structural characterisation technique. However, since electrons exhibit wave-like properties, the free electrons present in the crystal also experience the same diffraction phenomena, and this has a crucial effect on the spectrum of allowed electron energies. If we consider an electron wave travelling along a one dimensional chain of atoms of spacing a, then each atom will cause reflection of the wave. These reflections will all be constructive provided that $m\lambda=2a$, for integer m, where λ is the electron de Broglie wavelength (this is a special case of the Bragg Law of diffraction introduced in Section 2.1.2.5). When this condition is satisfied, both forward and backward travelling waves exist in the lattice, and the superposition of these creates standing waves. The standing waves correspond to electron density distributions $|\psi(x)|^2$ which have either all nodes, or all antinodes, at the lattice sites $x=a,\ 2a,\ 3a,\ldots$, and these two solutions, although having the same wavevector value, have quite different associated energies, due to the different interaction energies between the electrons and the positively charged ions. Consequently a *band gap* forms in the electron dispersion curve at the corresponding values of wavevector: $k=\pm m\pi/a$ (see figure 1.8). The fact that the electron waves are standing waves means that the electron group velocity

$$\nu_g=\frac{\partial\omega}{\partial k}=\frac{1}{\hbar}\frac{\partial E}{\partial k} \tag{1.11}$$

tends to zero at these points. This represents a fundamental difference between the behaviour of electrons in crystalline solids and that in free space, where the dispersion relationship remains purely parabolic ($E\propto k^2$) for all values of k.

The region of **k** space which lies between any two diffraction conditions is know as a Brillouin zone: thus, in a one-dimensional crystal, the first Brillouin zone lies between $k=-\pi/a$ and $k=+\pi/a$. However, any value of k which lies outside the first Brillouin zone corresponds, mathematically, to an electron wave of wavelength $\lambda<2a$. Such

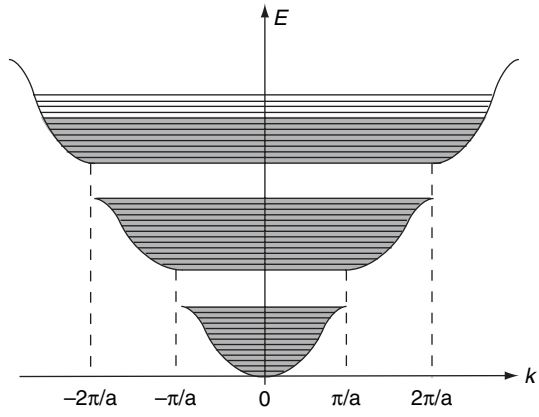

Figure 1.8 Schematic version of the parabolic relationship between the allowed electron wavevectors and the their energy for electrons confined to a one-dimensional potential well containing a periodically varying potential of period a. Shaded energy regions represent those occupied with electrons

a wave has too high a spatial frequency to be uniquely defined by a set of wave amplitudes which are only specified at lattice sites: an equivalent wave of wavelength $\lambda > 2a$ can always be identified. In **k**-space, this transformation is represented by the fact that any value of k lying outside the first Brillouin zone is equivalent to some point lying inside the first Brillouin zone, where the equivalent point is found from the relation

$$k' = k \pm 2m\pi/a \tag{1.12}$$

and the set of values $2m\pi/a$ are known as the reciprocal lattice vectors for the crystal.

In a three dimensional crystal, the location of energy gaps in the electron dispersion is still determined from electron diffraction by the lattice planes, but the Brillouin zones are no longer simple ranges of k, as in 1D: rather, they are described by complex surfaces in 3D **k**-space, the geometry of which depends on the unit cell and atomic structure. When the energy–wavevector relationship for such a crystal extending over multiple Brillouin zones is mapped entirely into the first Brillouin zone, as described above, this results in a large number of different energy bands and consequently the density of energy states takes on a very complex form. An example of the multiple energy bands and corresponding density of states in a real crystal is shown for the case of silicon in figure 1.9.

1.2.7 Electronic conduction

We may now observe that the series of allowed k values in equation 1.12 extends up to the edges of the Brillouin zone, at $k = \pm\pi/a$. Since one of these endpoints may be mapped onto the other by a reciprocal lattice vector translation, the total number of allowed k values is precisely N. Recalling that each k state may be occupied by both a spin up and a spin down electron, the total number of states available is $2N$ per energy band. In three dimensions, this result is generalised to $2N_u$ states per band, where N_u is the number of unit cells in the crystal. Now, the total number of valence electrons in the

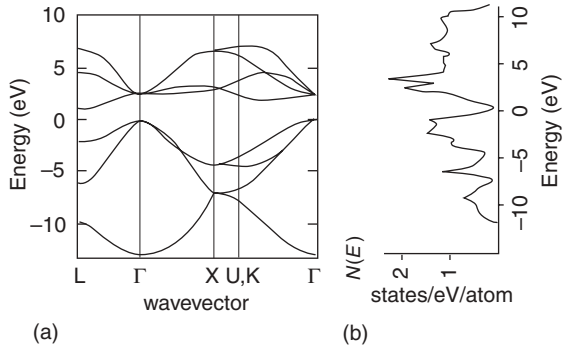

Figure 1.9 Electron energy band structure diagram and density of states for crystalline silicon. The symbols Γ, L, X, U and K on the horizontal (wavevector) axis of the band structure plot represent different symmetry points in 3D $\boldsymbol{k}$-space. Γ corresponds to $\boldsymbol{k} = \mathbf{0}$, the origin of the Brillouin zone; the range Γ–X represents a path through the Brillouin zone from centre to edge along the 100 direction; Γ–L and Γ–K represent middle to edge paths along the ⟨111⟩ and ⟨110⟩ directions, respectively, and X–U represents a path along the Brillouin zone boundary starting from the zone edge on the ⟨100⟩ axis and moving in a direction parallel to ⟨101⟩

crystal is zN_u, where z is the number of valence electrons per unit cell. This leads to two very different electronic configurations in a solid. If z is even, then one energy band is completely filled, with the next band being completely empty. The highest filled band is the valence band, and the next, empty band, is the conduction band. The electrons in the valence band cannot participate in electrical conduction, because there are no available states for them to move into consistent with the small increase in energy required by motion in response to an externally applied voltage: hence this configuration results in an insulator or, if the band gap is sufficiently small, a semiconductor. Alternatively, if z is odd, then the highest occupied energy band is only half full. In such a material, there are many vacant states immediately adjacent in energy to the highest occupied states, therefore electrical conduction occurs very efficiently and the material is a metal. Figure 1.10 shows schematic energy diagrams for insulators, metals and semiconductors respectively. There is one further, special case which gives rise to metallic behaviour: namely, when the valence band is completely full (z is even), but the valence and

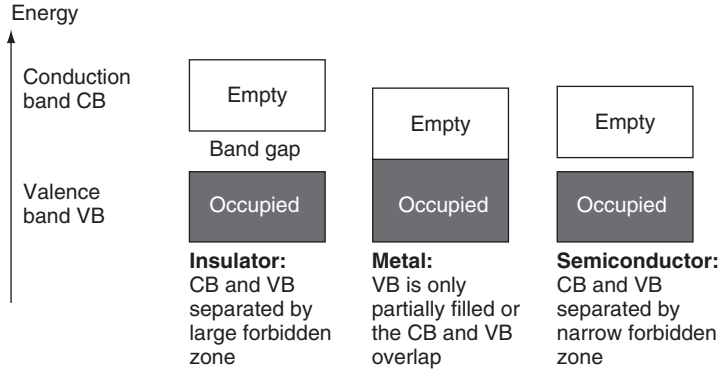

Figure 1.10 Electron energy band diagram for an insulator, a conductor and a semiconductor

conduction bands overlap in energy, such that there are vacant states immediately adjacent to the top of the valence band, just as in the case of a half-filled band. Such a material is called a semi-metal.

In the same way as was defined in the molecular orbital theory of section 1.2.3, the uppermost occupied energy level in a solid is the Fermi level E_F, and the corresponding Fermi wavevector is given by $E_F = \hbar k_F^2/2m_e$. As mentioned above, the volume of **k**-space per state is $8\pi^3/V$. Therefore, the volume of **k** space filled by N electrons is $4N\pi^3/V$, accounting for the fact that 2 electrons of opposite spins can occupy each wavevector state. If we equate this volume to the volume of a sphere in **k** space, of radius k_F (the Fermi sphere), we obtain the result

$$k_F = (3\pi^2 n_e)^{1/3} \tag{1.13}$$

where $n_e = N/V$ is the electron density, and hence

$$E_F = \hbar(3\pi^2 n_e)^{2/3}/2m_e. \tag{1.14}$$

If the Fermi sphere extends beyond the first Brillouin zone, as occurs in many metals, then the appropriate mapping back into the zone results in a Fermi surface of complex topology.

The density of states $N(E)dE$ is defined such that $N_s = \int N(E)dE$ gives the total number of states per unit crystal volume in an energy band. Now, from the above argument, the number of wavevector states per unit volume of **k** space is $V/8\pi^3$. Thus, the total number of states per band may be calculated from

$$N_s = 2 \times V/8\pi^3 \int d\mathbf{k} \tag{1.15}$$

where the factor of 2 accounts for the 2 spin states per **k** value. In three dimensions, $d\mathbf{k} = 4\pi k^2 dk$ and thus we may write

$$N_s = \frac{V}{4\pi^3} \int 4\pi k^2 \frac{dk}{dE} dE. \tag{1.16}$$

For parabolic bands, $E = \hbar^2 k^2/(2m_e)$ and hence $dk/dE = m_e/(\hbar^2 k)$, from which

$$N(E) = \frac{4\pi(2m_e)^{3/2}E^{1/2}}{h^3}. \tag{1.17}$$

The dependence of the density of states on $E^{1/2}(\propto k)$ is simply a consequence of the increased volume of phase space available at larger values of energy. The actual population of electrons as a function of energy is given by the product of the density of states and the occupation probability $f(E)$ which, for electrons or holes, is given by the Fermi Dirac function

$$f(E) = \frac{1}{\exp((E - E_F)/k_B T) + 1}, \tag{1.18}$$

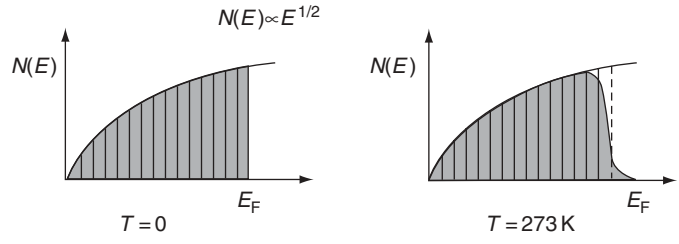

Figure 1.11 The density of electron states for free electrons and the occupation of electron energy levels (shaded region) at zero and room temperature

from which we may observe that the Fermi energy corresponds to the energy at which the occupation probability is exactly one half.

In the zero temperature limit, $f(E) = 1$ for all $E < E_F$, and $f(E) = 0$ for all $E > E_F$: in otherwords, all electron states below the Fermi energy are filled, and all those above E_F are empty, as previously described; the electron population at any energy $E < E_F$ is then given just by $N(E)$. At non-zero temperatures $f(E)$ describes the fact that some electrons are thermally excited from states just below E_F to states just above E_F, and the sharpness of the cut-off of $N(E)$ at E_F decreases with increasing temperature. Both zero temperature and non-zero temperature cases are shown in Figure 1.11.

In addition to the total DOS, which has already been mentioned, it is possible to project the DOS onto a particular atomic site in the unit cell and determine the so-called local DOS; this is the contribution of that particular atomic site to the overall electronic structure. If a unit cell contains a particular type of atom in two distinct crystallographic environments, then the local DOS will be correspondingly different. Similar projections may be performed in terms of the angular momentum symmetry (i.e., the s, p, d or f atomic character of the DOS).

Until now we have been concerned with crystalline systems. However, it is also possible to consider the DOS of an amorphous material; here the DOS is primarily determined by the short-range order in the material; i.e., the nearest neighbours. An alternative approach is to represent the amorphous solid by a very large unit cell with a large number of slightly different atomic environments.

1.3 EFFECTS OF THE NANOMETRE LENGTH SCALE

The small length scales present in nanoscale systems directly influence the energy band structure and can lead indirectly to changes in the associated atomic structure. Such effects are generally termed quantum confinement. The specific effects of quantum confinement in one, two and three dimensions on the density of states are discussed in detail in the Chapter 3 for the case of semiconductor nanostructures; however, initially we outline two general descriptions that can account for such size-dependent effects in nanoscale systems.

1.3.1 Changes to the system total energy

In the free electron model, it is clear that the energies of the electronic states depend on $1/L^2$ where L is the dimension of the system in that particular direction; the spacing between successive energy levels also varies as $1/L^2$. This behaviour is also clear from the description of a solid as a giant molecule: as the number of atoms in the molecule increases, the MOs gradually move closer together. Thus if the number of atoms in a system, hence the length scale, is substantially different to that in a normal bulk material, the energies and energy separations of the individual electronic states will be very different. Although in principle the Fermi level (Section 1.2.5) would not be expected to change since the free electron density N/V should remain constant, there may be associated modifications in structure (see below) which will change this quantity. Furthermore, as the system size decreases, the allowed energy bands become substantially narrower than in an infinite solid. The normal collective (i.e., delocalized) electronic properties of a solid become severely distorted and the electrons in a reduced-dimensional system tend to behave more like the 'particle in a box' description (Section 1.2.5); this is the phenomenon of quantum confinement. In otherwords, the electronic states are more like those found in localized molecular bonds rather than those in a macroscopic solid.

The main effect of these alterations to the bulk electronic structure is to change the total energy and hence, ignoring entropy considerations, the thermodynamic stability of the reduced length scale system relative to that of a normal bulk crystal. This can have a number of important implications. It may change the most energetically stable form of a particular material; for example, small nanoparticles or nanodimensional layers may adopt a different crystal structure from that of the normal bulk material. For example, some metals which normally adopt a hexagonal close-packed atomic arrangement have been reported to adopt a face-centred cubic structure in confined systems such as metallic multilayers. If a different crystallographic structure is adopted below some particular critical length scale, then this arises from the corresponding change in the electronic density of states which often results in a reduced total energy for the system.

Reduction of system size may change the chemical reactivity, which will be a function of the structure and occupation of the outermost electronic energy levels. Correspondingly, physical properties such as electrical, thermal, optical and magnetic characteristics, which also depend on the arrangement of the outermost electronic energy levels, may be changed. For example, metallic systems can undergo metal–insulator transitions as the system size decreases, resulting from the formation of a forbidden energy band gap. Other properties such as mechanical strength which, to a first approximation, depends on the change in electronic structure as a function of applied stress and hence interatomic spacing, may also be affected. Transport properties may also change in that they may now exhibit a quantized rather than continuous behaviour, owing to the changing nature and separation of the electron energy levels.

1.3.2 Changes to the system structure

A related viewpoint for understanding the changes observed in systems of reduced dimension is to consider the proportion of atoms which are in contact with either a

free surface, as in the case of an isolated nanoparticle, or an internal interface, such as a grain boundary in a nanocrystalline solid. Both the surface area to volume ratio (S/V) and the specific surface area (m^2g^{-1}) of a system are inversely proportional to particle size and both increase drastically for particles less than 100 nm in diameter. For isolated spherical particles of radius r and density ρ, the surface area per unit mass of material is equal to $4\pi r^2/(4/3\pi r^3\rho) = 3/r\rho$. For 2 nm diameter spherical particles of typical densities, the specific surface area (SSA) can approach $500\,m^2\,g^{-1}$. However, for particles in contact this value will be reduced by up to approximately half. This large surface area term will have important implications for the total energy of the system. As discussed above this may lead to the stabilization of metastable structures in nanometre-sized systems, which are different from the normal bulk structure or, alternatively, may induce a simple relaxation (expansion or contraction) of the normal crystalline lattice which could in turn alter other material properties.

If an atom is located at a surface then it is clear that the number of nearest-neighbour atoms are reduced, giving rise to differences in bonding (leading to the well-known phenomenon of surface tension or surface energy) and electronic structure. In a small isolated nanoparticle, a large proportion of the total number of atoms will be present either at or near the free surface. For instance, in a 5 nm particle approximately 30–50% of the atoms are influenced by the surface, compared with approximately a few percent for a 100 nm particle. Similar arguments apply to nanocrystalline materials, where a large proportion of atoms will be either at or near grain boundaries. Such structural differences in reduced-dimensional systems would be expected to lead to very different properties from the bulk.

1.3.2.1 Vacancies in nanocrystals

Another important consideration for nanostructures concerns the number of atomic vacancies n_v which exist in thermal equilibrium in a nanostructure. Vacancies are point defects in the crystalline structure of a solid and may control many physical properties in materials such as conductivity and reactivity. In microcrystalline solids at temperatures above 0 K, vacancies invariably exist in thermal equilibrium. In the simple case of metals with one type of vacancy, the number of vacancies in a crystal consisting of N atom sites is approximated by an Arrhenius-type expression

$$n_v = N\exp(-Q_f/RT), \tag{1.19}$$

where T is the absolute temperature, R is the gas constant and Q_f is the energy required to form one mole of vacancies. Q_f is given by the relationship $Q_f = N_A q_f$, where N_A is the Avogadro number and q_f is the activation energy for the formation of one vacancy. However, the value of q_f is not well defined but is generally estimated to be the energy required to remove an atom from the bulk interior of a crystal to its surface. As a rough approximation, a surface atom is bonded to half the number of atoms compared with an interior atom, so q_f represents half the bonding energy per atom. Since the melting temperature T_m of a metal is also a measure of the bond energy, then q_f is expected to be a near linear function of T_m.

From a continuum model, Q_f may be estimated from the latent heat of vaporisation, since on leaving the surface an atom breaks the remaining (half) bonds. In practice it is found that the latent heat of vaporisation is considerably higher than Q_f. Alternatively, Q_f may be estimated from the surface energy per unit area. Given that one atom occupies an area b^2, the number of atoms per unit area is equal to $1/b^2$ and the surface energy σ is therefore q_f/b^2. Surface energies depend on melting temperature and vary within the range $1.1\,J\,m^{-2}$ (for aluminium) to $2.8\,J\,m^{-2}$ (for tungsten). Taking an average value of σ as $2.2\,J\,m^{-2}$ and $b = 2.5 \times 10^{-10}$ m, we may calculate $Q_f = N_A \sigma b^2$ as $83 \times 10^3\,J\,mol^{-1}$, which is close to the accepted value of $90\,kJ\,mol^{-1}$.

Furthermore, the value of Q_f may be modified for nanoparticles through the influence of the surface energy term, σ, which is related to the internal pressure, P, by the simple relationship $P = 4\sigma/d$, where d is the diameter of the nanoparticle. The effect of P is to require an additional energy term, q_n, for the formation of a vacancy, which is approximately given by Pb^3. Again taking σ as $2.2\,J\,m^{-2}$, we may calculate this additional energy per mole $Q_n = N_A q_n$ as $8.3 \times 10^3\,J\,mol^{-1}$ for a 10 nm diameter nanoparticle. This term is only approximately 10% of Q_f and rapidly decreases for larger particle sizes. Thus we may conclude that the effect of the surface energy (internal pressure) factor on the vacancy concentration will be small. Additionally, the internal pressure P results in an elastic, compressive volume strain, and hence linear strain, ε, given approximately as

$$\varepsilon = P/3E = 4\sigma/3dE \tag{1.20}$$

where E is the Young's modulus. This expression suggests that the linear strain will be inversely proportional to particle size and that there will be a decrease in lattice parameter or interatomic spacing for small nanoparticles. This prediction correlates reasonably well with the data in Figure 1.12.

Finally, substituting a value of $Q_f = 90 \times 10^3\,J\,mol^{-1}$ into the Arrhenius expression (1.19) for the vacancy concentration, we obtain values for the ratio n_v/N of 2.4×10^{-16} (at 300 K), 6.5×10^{-7} (at 600 K) and 4.8×10^{-4} (at 1000 K), illustrating the exponential

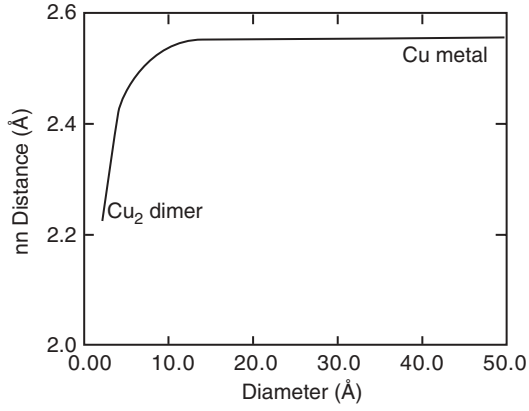

Figure 1.12 Schematic diagram of the change in nearest-neighbour (nn) distance as a function of cluster size or particle size for copper

increase in vacancy concentration with temperature. Now consider a spherical nanoparticle, say 50 nm in diameter, and in which each atom occupies a volume b^3. Again taking $b = 0.25$ nm, there are a total of 4.2×10^6 atoms in the particle, which implies that $n_v << 1$, except at very high temperatures. Therefore nanocrystals are predicted to be essentially vacancy-free; their small size precludes any significant vacancy concentration. This simple result also has important consequences for all thermomechanical properties and processes (such as creep and precipitation) which are based on the presence and migration of vacancies in the lattice.

1.3.2.2 Dislocations in nanocrystals

Planar defects, such as dislocations, in the crystalline structure of a solid are extremely important in determining the mechanical properties of a material. It is expected that dislocations would have a less dominant role to play in the description of the properties of nanocrystals than in the description of the properties of microcrystals, owing to the dominance of crystal surfaces and interfaces. The free energy of a dislocation is made up of a number of terms: (i) the core energy (within a radius of about three lattice planes from the dislocation core); (ii) the elastic strain energy outside the core and extending to the boundaries of the crystal, and (iii) the free energy arising from the entropy contributions. In microcrystals the first and second terms increase the free energy and are by far the most dominant terms. Hence dislocations, unlike vacancies, do not exist in thermal equilibrium.

The core energy is expected to be independent of grain size. Estimates are close to 1 eV per lattice plane which, for an interplanar spacing b of 0.25 nm, translates to a value of about 6.5×10^{-10} J m^{-1}. The elastic strain energy per unit length for an edge dislocation is given by

$$E = \frac{Gb^2}{4\pi(1-\nu)} \times \ln\left(\frac{r_1}{r_0}\right) \tag{1.21}$$

where G is the bulk modulus, r_0 is the core radius, r_1 is the crystal radius and ν is Poisson's ratio. ν is typically around 1/3 for a crystalline sample. The expression for a screw dislocation omits the $(1-\nu)$ term, giving an energy about 2/3 that of an edge dislocation. For $G = 40 \times 10^9$ Pa, the constant term $Gb^2/4\pi(1-\nu)$ has a value of 3×10^{-10} J m^{-1}. The grain size dependence is given in the $\ln(r_1/r_0)$ term, which for grain size $(2r_1)$ values of 10, 50, 1000 and 10 000 nm increases as 3, 4.6, 7.6 and 9.9 respectively. Hence it can be seen that the elastic strain energy of dislocations in nanoparticles and nanograined materials is about one-third of that in microcrystals and that, for a 10 nm grain size the core energy is comparable with the elastic strain energy. In comparison, the core energy is about one-tenth of the elastic strain energy for a microcrystal.

This reduction in the elastic strain energy of dislocations in nanocrystals has important consequences. The forces on dislocations due to externally applied stresses are reduced by a factor of about three and the interactive forces between dislocations are reduced by a factor of about 10. Hence recovery rates and the annealing out of dislocations to free surfaces are expected to be reduced. For a dislocation near the surface of a semi-infinite solid, the stress towards the surface is given by the interaction

of the stress field of an image dislocation at an equal distance on the opposite side. Since nanocrystals do not approximate to semi-infinite solids, such image stresses will operate across all surfaces and the net effect, together with the reduced elastic strain energy, results in dislocations that are relatively immobile.

Finally, we estimate the entropy contributions to the free energy. These arise as a result of (i) configurational entropy (i.e., the dislocation can be arranged in a variety of ways), (ii) a further contribution if the dislocation is assumed to be perfectly flexible, and (iii) the effect of the dislocation on the thermal vibrations of the crystal. Factors (ii) and (iii) are independent of crystal size and their values can be estimated to be $2k_BT$ and $3k_BT$, respectively, per atomic plane. Assuming a temperature of 300 K, these values correspond to about $3 \times 10^{-11}\,\mathrm{J\,m^{-1}}$, considerably less than the core and elastic strain energy terms. The configurational entropy contribution to the free energy is given by

$$E = \frac{bk_BT}{L}\ln\left(\frac{L^2}{b^2}\right) \tag{1.22}$$

per atom plane, where L is the length of the dislocation. At 300 K this gives values of $3.0 \times 10^{-12}, 5.7 \times 10^{-14}$ and $7.6 \times 10^{-15}\,\mathrm{J\,m^{-1}}$ for $L = 10$, 1000 and 10 000 nm, respectively. These values are again much smaller than the core and elastic strain energy terms and hence it may be concluded that dislocations in nanocrystals, as with microcrystals, do not exist as thermodynamically stable lattice defects.

1.3.3 How nanoscale dimensions affect properties

Many properties are continuously modified as a function of system size. Often these are extrinsic properties, such as resistance, which depend on the exact size and shape of the specimen. Other properties depend critically on the microstructure of the material; for example, the Hall–Petch equation for yield strength, σ, of a material as a function of average grain size $\langle d \rangle$ is given by

$$\sigma = k\langle d \rangle^{-1/2} + \sigma_0 \tag{1.23}$$

where k and σ_0 are constants. Intrinsic materials properties, such as resistivity, should be independent of specimen size, however, even many of the intrinsic properties of matter at the nanoscale are not necessarily predictable from those observed at larger scales. As discussed above this is because totally new phenomena can emerge, such as: quantum size confinement leading to changes in electronic structure; the presence of wave-like transport processes, and the predominance of interfacial effects.

1.3.3.1 Structural properties

The increase in surface area and surface free energy with decreasing particle size leads to changes in interatomic spacings. For Cu metallic clusters the interatomic spacing is observed to decrease with decreasing cluster size, as shown in Figure 1.12. This effect

can be explained by the compressive strain induced by the internal pressure arising from the small radius of curvature in the nanoparticle (Section 1.3.2.2). Conversely, for semiconductors and metal oxides there is evidence that interatomic spacings increase with decreasing particle size.

A further effect, previously mentioned, is the apparent stability of metastable structures in small nanoparticles and clusters, such that all traces of the usual bulk atomic arrangement become lost. Metallic nanoparticles, such as gold, are known to adopt polyhedral shapes such as cube–octahedra, multiply twinned icosahedra and multiply twinned decahedra (Figure 1.13). These nanoparticles may be regarded as multiply twinned crystalline particles (MTPs) in which the shapes can be understood in terms of the surface energies of various crystallographic planes, the growth rates along various crystallographic directions and the energy required for the formation of defects such as twin boundaries. However, there is compelling evidence that such particles are not crystals but are quasiperiodic crystals or crystalloids. These icosahedral and decahedral quasicrystals form the basis for further growth of the nanocluster, up until a size where they will switch into more regular crystalline packing arrangements.

Crystalline solids are distinct from amorphous solids in that they possess long-range periodic order and the patterns and symmetries which occur correspond to those of the 230 space groups. Quasiperiodic crystals do not possess such long-range periodic order and are distinct in that they exhibit fivefold symmetry, which is forbidden in the 230 space groups. In the cubic close-packed and hexagonal close-packed structures, exhibited by many metals, each atom is coordinated by 12 neighbouring atoms. All of the coordinating atoms are in contact, although not evenly distributed around the central atom. However, there is an alternative arrangement in which each coordinating atom is situated at the apex of an icosahedron and in contact only with the central atom. If however we relax this 'rigid atomic sphere' model and allow the central atom to reduce in diameter by 10%, the coordinating atoms come into contact and the body now has the shape and symmetry of a regular icosahedron with point group symmetry 235, indicating the presence of 30 twofold, 20 threefold and 12 fivefold axes of symmetry. This geometry represents the nucleus of a quasiperiodic crystal which may grow in the forms of icosahedra or pentagonal dodecahedra. These are dual solids with identical symmetry, the apices of one being replaced by the faces of the other. Such quasiperiodic crystals are known to exist in an increasing number of aluminium-based alloys and may be stable up to microcrystalline sizes. It should be noted that their symmetry is precisely the same as that of the fullerenes C_{20} (dodecahedrene with 12 pentagonal faces of a pentagonal dodecahedron, but unstable) and C_{60} (the well-known buckyball with 12 pentagonal faces and 20 hexagonal faces of a truncated icosahedron). Hence, like the fullerenes, quasiperiodic crystals are expected to have an important role to play in nanostructures.

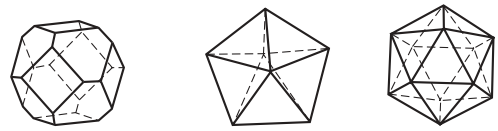

Figure 1.13 Geometrical shapes of cubo-octahedral particles and multiply twinned decahedral and icosahedral particles

The size-related instability characteristics of quasiperiodic crystals are not well understood. A frequently observed process appears to be that of multiple twinning, such crystals being distinguished from quasiperiodic crystals by their electron diffraction patterns. Here the five triangular faces of the fivefold symmetric icosahedron can be mimicked by five twin-related tetrahedra (with a close-packed crystalline structure) through relatively small atomic movements.

1.3.3.2 Thermal properties

The large increase in surface energy and the change in interatomic spacing as a function of nanoparticle size mentioned above have a marked effect on material properties. For instance, the melting point of gold particles, which is really a bulk thermodynamic characteristic, has been observed to decrease rapidly[2] for particle sizes less than 10 nm, as shown in Figure 1.14. There is evidence that for metallic nanocrystals embedded in a continuous matrix the opposite behaviour is true; i.e., smaller particles have higher melting points.[3]

1.3.3.3 Chemical properties

The change in structure as a function of particle size is intrinsically linked to the changes in electronic properties. The ionization potential (the energy required to remove an electron) is generally higher for small atomic clusters than for the corresponding bulk material. Furthermore, the ionization potential exhibits marked fluctuations as a function of cluster size. Such effects appear to be linked to chemical reactivity, such as the reaction of Fe_n clusters with hydrogen gas (Figure 1.15).

Nanoscale structures such as nanoparticles and nanolayers have very high surface area to volume ratios and potentially different crystallographic structures which

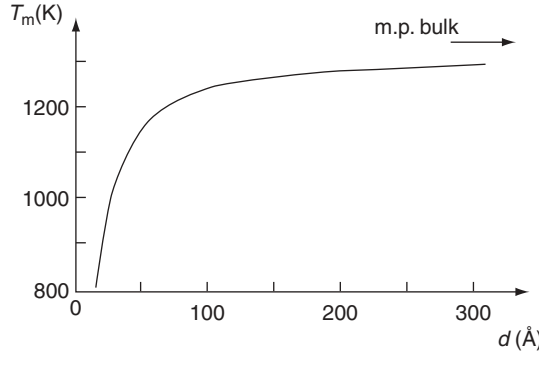

Figure 1.14 Schematic diagram of the variation in melting point of gold nanoparticles as a function of particle size

[2] *Nanomaterials: Synthesis, Properties and Applications*, ed. A. S. Edelstein and R. C. Cammarata (Institute of Physics 1996) and references therein.
[3] U. Dahmen *et al.*, *Inst.Phys. Conf. Ser.* **168**, 1 (IOP Publishing 2001).

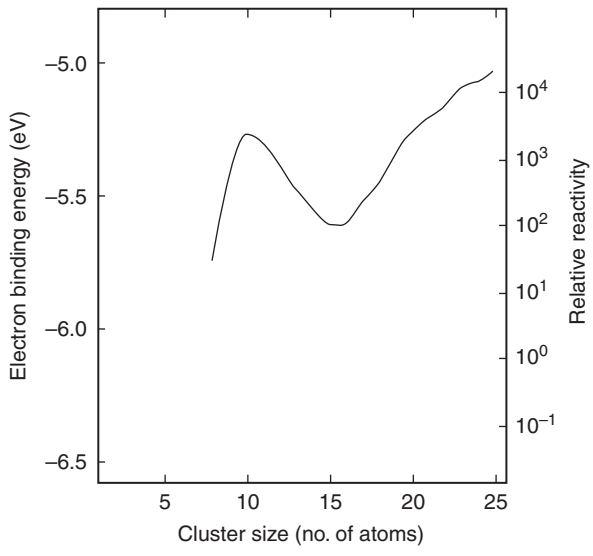

Figure 1.15 Schematic diagram of the dependence of the electron binding energy and relative chemical reactivity of iron clusters to hydrogen gas as a function of cluster size

may lead to a radical alteration in chemical reactivity. Catalysis using finely divided nanoscale systems can increase the rate, selectivity and efficiency of chemical reactions such as combustion or synthesis whilst simultaneously significantly reducing waste and pollution. Gold nanoparticles smaller than about 5 nm in diameter are known to adopt icosahedral structures rather than the normal face centred cubic arrangement. This structural change is accompanied by an extraordinary increase in catalytic activity. Furthermore, nanoscale catalytic supports with controlled pore sizes can select the products and reactants of chemical reactions based on their physical size and thus ease of transport to and from internal reaction sites within the nanoporous structure. Additionally, nanoparticles often exhibit new chemistries as distinct from their larger particulate counterparts; for example, many new medicines are insoluble in water when in the form of micron-sized particles but will dissolve easily when in a nanostructured form.

1.3.3.4 Mechanical properties

Many mechanical properties, such as toughness, are highly dependent on the ease of formation or the presence of defects within a material. As the system size decreases, the ability to support such defects becomes increasingly more difficult and mechanical properties will be altered accordingly. Novel nanostructures, which are very different from bulk structures in terms of the atomic structural arrangement, will obviously show very different mechanical properties. For example, single- and multi-walled carbon nanotubes show high mechanical strengths and high elastic limits that lead to considerable mechanical flexibility and reversible deformation.

As the structural scale reduces to the nanometre range, for example, in nanoayered composites, a different scale dependence from the usual Hall–Petch relationship

(Equation 1.23) for yield strength often becomes apparent with large increases in strength reported. In addition, the high interface to volume ratio of consolidated nanostructured materials appears to enhance interface-driven processes such as plasticity, ductility and strain to failure. Many nanostructured metals and ceramics are observed to be superplastic, in that they are able to undergo extensive deformation without necking or fracture. This is presumed to arise from grain boundary diffusion and sliding, which becomes increasingly significant in a fine-grained material. Overall these effects extend the current strength–ductility limit of conventional materials, where usually a gain in strength is offset by a corresponding loss in ductility.

1.3.3.5 Magnetic properties

Magnetic nanoparticles are used in a range of applications, including ferrofluids, colour imaging, bioprocessing, refrigeration as well as high storage density magnetic memory media. The large surface area to volume ratio results in a substantial proportion of atoms (those at the surface which have a different local environment) having a different magnetic coupling with neighbouring atoms, leading to differing magnetic properties. Figure 1.16 shows the magnetic moments of nickel nanoparticles as a function of cluster size.

Whilst bulk ferromagnetic materials usually form multiple magnetic domains, small magnetic nanoparticles often consist of only one domain and exhibit a phenomenon known as superparamagnetism. In this case the overall magnetic coercivity (Section 4.1) is then lowered: the magnetizations of the various particles are randomly distributed due to thermal fluctuations and only become aligned in the presence of an applied magnetic field.

Giant magnetoresistance (GMR) is a phenomenon observed in nanoscale multi-layers consisting of a strong ferromagnet (e.g., Fe, Co) and a weaker magnetic or non-magnetic buffer (e.g., Cr, Cu); it is usually employed in data storage and sensing. In the absence of a magnetic field the spins in alternating layers are oppositely aligned through antiferromagnetic coupling, which gives maximum scattering from the interlayer interface and hence a high resistance parallel to the layers. In an

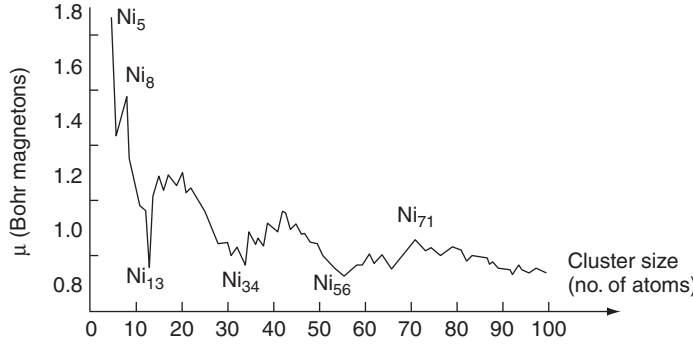

Figure 1.16 Schematic diagram of the variation in magnetic moments of clusters as a function of cluster size. The Bohr magneton is the classical magnetic moment associated with an electron orbiting a nucleus which has a single positive charge

oriented external magnetic field the spins align with each other and this decreases scattering at the interface and hence resistance of the device. Further details are given in Chapter 4.

1.3.3.6 Optical properties

In small nanoclusters the effect of reduced dimensionality on electronic structure has the most profound effect on the energies of the highest occupied molecular orbital (HOMO), essentially the valence band, and the lowest unoccupied molecular orbital (LUMO), essentially the conduction band. Optical emission and absorption depend on transitions between these states; semiconductors and metals, in particular, show large changes in optical properties, such as colour, as a function of particle size. Colloidal solutions of gold nanoparticles have a deep red colour which becomes progressively more yellow as the particle size increases; indeed gold colloids have been used as a pigment for stained glass since the seventeenth century. Figure 1.17 shows optical absorption spectra for colloidal gold nanoparticles of varying sizes. Semiconductor nanocrystals in the form of quantum dots show similar size-dependent behaviour in the frequency and intensity of light emission as well as modified non-linear optical properties and enhanced gain for certain emission energies or wavelengths. Other properties which may be affected by reduced dimensionality include photocatalysis, photoconductivity, photoemission and electroluminescence.

1.3.3.7 Electronic properties

The changes which occur in electronic properties as the system length scale is reduced are related mainly to the increasing influence of the wave-like property of the electrons (quantum mechanical effects) and the scarcity of scattering centres. As the size of the

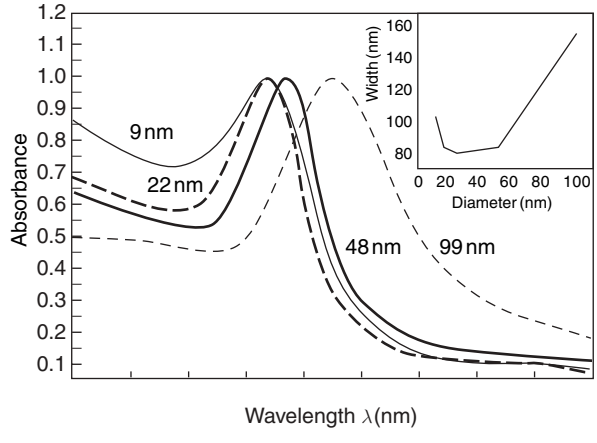

Figure 1.17 Size dependence of the optical absorption wavelength for gold nanoparticles and (inset) the corresponding value of the full width at half maximum (FWHM) of the absorption peak